A 117-W 1.66-Times Diffraction Limited Continuous-Wave Nd:YVO_4 Zigzag Slab Laser with Multilayer Amplified-Spontaneous-Emission Absorbing Coatings *

Zhi-Feng Zhang(张志峰)[1,2], Shuai Li(李帅)[3], Yang Li(李阳)[2], Yang Kou(寇洋)[2], Ke Liu(刘可)[2], Yan-Yong Lin(林延勇)[2], Lei Yuan(袁磊)[2], Yi-Ting Xu(徐一汀)[2]**, Qin-Jun Peng(彭钦军)[2], Zu-Yan Xu(许祖彦)[2]

[1] *University of Chinese Academy of Sciences, Beijing 100190, China*
[2] *Key Laboratory of Solid-State Laser, Technical Institute of Physics and Chemistry, Chinese Academy of Sciences, Beijing 100190, China*
[3] *Beijing Aerocim Technology Co., Ltd, Beijing 100043, China*

(Received 10 March 2020)

We report a continuous-wave end-pumped Nd:YVO_4 zigzag slab laser with multilayer amplified spontaneous emission (ASE) absorbing coatings. The coatings are deposited on the slab faces. A five-layer structure consists of SiO_2-Ti-SiO_2-Ti-Au, and the thicknesses are 2520 nm, 10 nm, 160 nm, 24 nm and 200 nm, respectively. The designed coatings show good performance for the ASE control in the experimental tests. A stable-unstable hybrid laser oscillator along orthogonal directions in the slab aperture is further configured, achieving the 117 W output at a pump of 328 W. The beam quality factors M^2 in the unstable direction and stable direction are 1.57 and 1.66, respectively.

PACS: 42.55.Xi, 42.60.Da, 42.60.Pk DOI: 10.1088/0256-307X/37/6/064203

Many applications, such as optical communication, navigation systems, biotechnology, and laser medicine, demand compact, high power, and high beam quality polarized lasers.[1–3] Laser diode (LD) end-pumped rod solid-state laser has been a focus of development in the past decade. However, the output power is limited by thermally induced lensing and fracture damage. To further achieve high power, high beam quality polarized output, the InnoSlab and other multipass structures were developed by different groups. Among widely used neodymium-doped crystals, the Nd:YVO_4 has a stimulated emission cross section five times larger than that of Nd:YAG, and its large birefringence is favorable to polarized laser oscillation. Nevertheless, vanadate's relatively poor thermal and mechanical characteristic limits the pump power. To reduce the thermal load of the crystal, the efficient "four-level laser" pump scheme with direct pumping to the upper lasing level was investigated.[2,4,5] However, it only improves laser performance slightly. Therefore, the laser configurations with better thermal dissipation capability are demanded. It is well-known that the conduction-cooled end-pumped zigzag slab configuration is featured by the uniform pump, the high cooling capability, and the zigzag optical path that averages the thermo-optic effect.[6–8] Unfortunately, ASE is a critical factor that limits the performance of the Nd:YVO_4 zigzag slab lasers.[6,9–11] The ASE issue is severe due to the large stimulated emission cross section of Nd:YVO_4 and the long optical path of zigzag propagation. The severe ASE in Nd:YVO_4 zigzag slab hinders the laser from getting higher power. Although the ASE could be utilized in some applications such as superluminescent diodes (SLDs) and superfluorescent source (SFS),[12,13] the ASE in zigzag slab lasers is undesirable. The management of ASE in zigzag slab lasers is of significant importance for high power, high beam quality output. Fortunately, the ASE could be managed efficiently by special designed absorbing coatings. Dobrowolski's group proved that using metal/dielectric films could make broadband absorption coatings.[14,15]

In this Letter, as for the zigzag structure that Nd:YVO_4 slab lasers rarely adopt because of the severe ASE, we solve the problem with designed absorbing coatings. A conduction-cooled double-end-pumped Nd:YVO_4 zigzag slab laser with a hybrid resonator is proposed. The proposed scheme has both the features of the high overlapping efficiency and excellent cooling capability.[16,17] The 888 nm pumping light is used to reduce the heat load of the slab further. The ASE effect is successfully managed with specially designed absorbing coatings. The experimental scheme discussed would support the development of high-power Nd:YVO_4 zigzag slab lasers technically.

The Nd:YVO_4 slab used in our experiments has dimensions of 45 mm × 12 mm × 1.2 mm, as shown in Fig. 1(a). The slab was a-cut in the length direction and c-cut along the width direction. The slab contains a doped region that diffusely bonded to un-doped end caps. The doped region of Nd:YVO_4 slab crystal was 0.5 at.% doped concentration, and the un-doped end

*Supported by the National Key R&D of China (Grant No. 2016YFB0402103), the National Natural Science Foundation of China (Grant No. 61875208), and the Knowledge Innovation Program of Chinese Academy of Sciences (Grant No. GJJSTD20180004).
**Corresponding author. Email: ytxu@mail.ipc.ac.cn
© 2020 Chinese Physical Society and IOP Publishing Ltd

caps were cut into a trapezoidal sample. The two cut edge facets formed an angle of 45° with respect to the bottom surface, and the facet coatings were anti-reflective (AR) at 1064 nm and high-reflective (HR) at 888 nm.

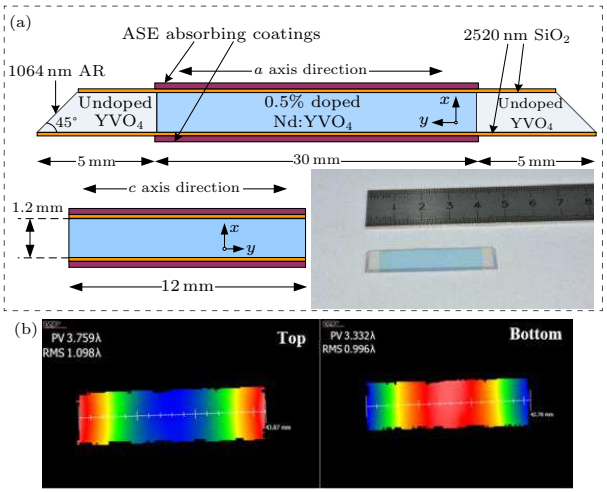

Fig. 1. (a) Two-dimensional view of the slab. (b) The measured surface shape of the two large surfaces from the Zygo interferometer.

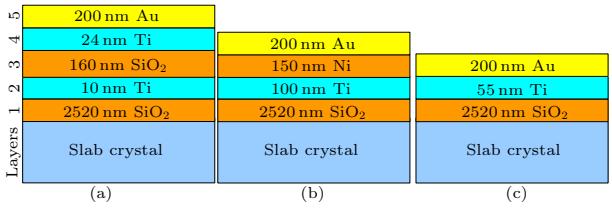

Fig. 2. (a) The five-layer coating structure, (b) four-layer coating structure, and (c) three-layer coating structure.

The pump was absorbed along the length of the doped region and the large surfaces of the slab provided the zigzag propagation with total internal reflection (TIR) for the 1064 nm laser beam. The laser beam was incident at a near-normal angle to the end faces. The shapes of the two large surfaces were measured by the Zygo interferometer, and the results are shown in Fig. 1(b). The PV and RMS of the two surfaces were 3.76λ, 1.10λ, 3.33λ, and 1.00λ (@632.8 nm), respectively.

The detailed designs of coating structures are presented in Fig. 2. At the bottom, a 2520-nm-thick SiO_2 coating was deposited on the large surfaces. The SiO_2 coating has three distinct and independent functions. Firstly, it ensured the TIR zigzag reflections of the laser. Secondly, it achieved an AR coating function for the pumping light wavelength when the end-pumped light passed through the bottom surface, as shown in Fig. 3. Last but not least, it made the ASE light AR and incident to the absorbing coatings. The absorbing coatings were deposited on the 2520 nm SiO_2 film and composed by Ti and SiO_2 films of different thicknesses. The refractive index of the Ti films is a complex quantity when the thickness is smaller than the wavelength of incident radiation. Thus, the stray light will be absorbed by Ti films when it entered the absorbing coatings, and the SiO_2 film acted as an AR coating. The 200 nm Au film was made to match with the indium solder. Then two large surfaces of the crystal were soldered to heat sinks with indium solder carefully to maintain high stability and thermal conductivity of the slab module. The thickness of the film was optimized by the Essential Macleod Program.

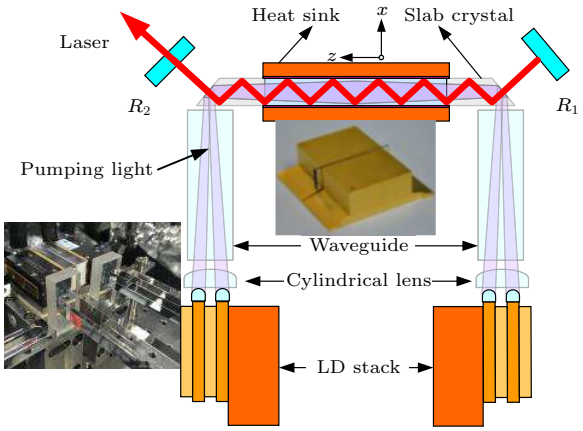

Fig. 3. Experimental setup to test different ASE absorbing coatings.

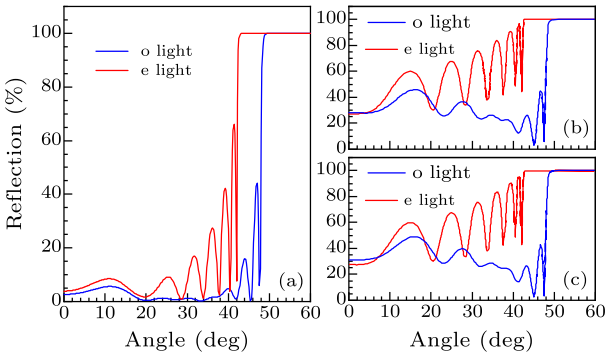

Fig. 4. Dependence of the reflectivity for 1064 nm ordinary light and extraordinary light as a function of the incidence angle of stray light from slab crystal to coatings: (a) five layers, (b) four layers, (c) three layers.

Because θ_{ce} and θ_{co} are different, by adjusting the incident angle, we can achieve that only e light oscillates in the resonator. Therefore, the incident angle θ of the laser beam inside the slab was designed between $\theta_{ce} = 42.1°$ and $\theta_{co} = 47.9°$ with respect to the normal vector of the reflection surface. Take Fig. 2(a) as an example, for the e light, the reflectivity did not exceed 10% when the incident angle ranged from 0° to 30°. When the incident angle ranged from 30° to $\theta_{ce} = 42.1°$, the reflectivity exceeded 50% only at an incident angle around 41.4°. The other two cases, however, have higher reflection (both o light and e light) even with very a small incident angle, as shown in Figs. 4(b) and 4(c). The coating structure in Fig. 2(a) may have the best performance concluded from Fig. 4.

To test the design of the ASE absorbing coatings shown in Fig. 2, a stable plane concave resonator with $R_1 = 700$ mm and $T = 40\%$ was configured as schematically shown in Fig. 3. Three Nd:YVO_4 slab modules were developed with ASE absorbing coatings corresponding to Fig. 2.

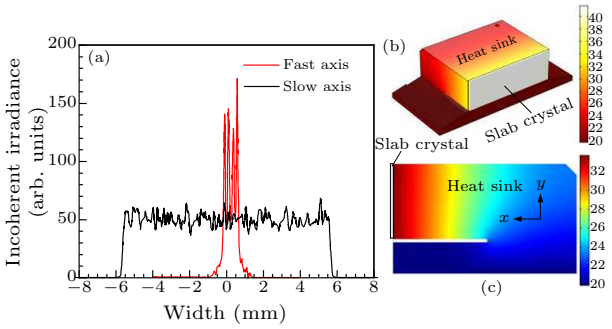

Fig. 5. (a) Pump light intensity distribution at slab entrance; (b) and (c) the calculated temperature distribution of the heat sink.

The pumping unit consisted of two stacks, and each stack had two laser diode bars. The central output wavelength of the pumping unit was 888 nm, and the spectral width of the laser diode stack was about 3 nm. The LD was 11.5 mm width in the slow axis direction with a divergence angle of 10°. In the fast axis direction, the radiation from each laser diode bar was collimated with micro-lens and the divergence angle can be significantly decreased to 0.1°. The collimated beam was focused into the rectangular waveguide by a cylindrical lens with a focal length of 300 mm in the fast axis direction. The planar waveguides were 300 mm long and 11.5 mm ×11.5 mm in the fast and slow axial directions. The divergence angle was maintained within 10° at the output end of the planar waveguide in the slow axial direction. With this pumping unit, we obtained a homogeneous pumping line with dimensions of ∼1.1 mm ×11.5 mm at each end of Nd:YVO_4 slab, as shown in Fig. 5(a). The Nd:YVO_4 slab module was conduction-cooled and the slab was soldered between two gold plating heat sinks with indium. The thickness of the indium was 0.4 mm, and the structure was optimized by the finite element method (FEM), as shown in Figs. 5(b) and 5(c). The thermal load was set to be 95 W in simulations. It could be seen that the temperature was uniformly distributed, as shown in Fig. 5(b), and the temperature difference was within 0.2 ℃, as shown in Figs. 5(b) and 5(c). The temperature difference was within 0.4 ℃ in experiments monitored by the infrared radiation thermal sensor.

The output power versus the absorbed pump power of different coating structures in short-cavity experiments is illustrated in Fig. 6(a). The curves marked with a, b, and c correspond to the designed absorbing coatings in Fig. 2, respectively. In situation c (the blue curve), it has the lowest efficiency and the output power decreased when the pump beyond 200 W, as shown in Fig. 6(a). In situation b (the red curve), the absorbing coatings were composed of Ti and Ni films of different thicknesses, and the output power was simply 65 W at the pump level of 238 W, corresponding to the optical-to-optical (O-O) efficiency of 27.3%. Further increasing pump led to the temperature rise in the slab. In situation a (the black curve), the O-O efficiency was 47.5%, and the slope efficiency was as high as 68%. In addition, the output curve shows no evidence of saturation. The test results show that the coating structure designed in Fig. 2(a) was efficient in managing the ASE in Nd:YVO_4 slabs. Thus the coating structure in (a) was adopted in the last. The experiment results are in accordance with the coating designs shown in Fig. 4. The wavefront of the Nd:YVO_4 slab without the pump and with 322 W pump (corresponding to 153 W output) are shown in Figs. 6(b) and 6(c). The slight variations in RMS and PV indicate that the slab has good thermal management.

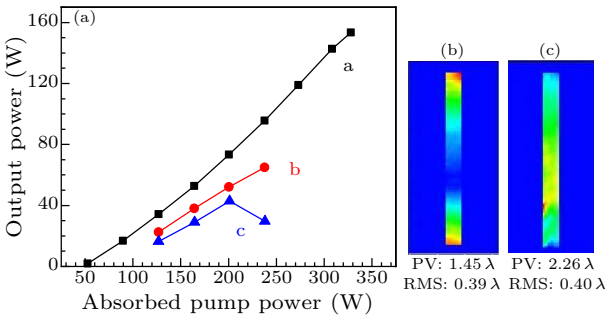

Fig. 6. (a) Output power versus the absorbed pump power of different coating structures in short-cavity experiments. (b) Wavefront without the pump. (c) Wavefront with 153 W output.

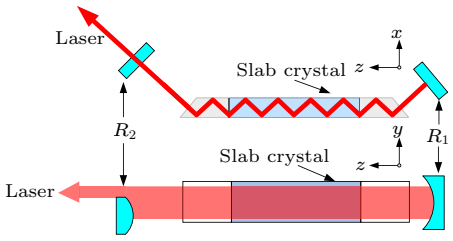

Fig. 7. Schematic diagram of the unstable-stable hybrid resonator.

A hybrid resonator, stable direction in thickness and unstable direction in width, was configured experimentally to obtain high power, high beam quality laser. A schematic diagram of the positive branch unstable-stable hybrid resonator is shown in Fig. 7. Two highly reflective cylindrical mirrors, M1 ($R_1 = -1000$ mm) and M2 ($R_2 = 650$ mm), were used as the resonator mirrors. The cavity length was about 175 mm, and the distances between R_1/R_2 to the end face were 20 mm/125 mm. A positive-branch confocal off-axis unstable resonator with magnification $M = 1.5$ was formed in the y–z plane, correspond-

ing to an output coupling $T = 35\%$. A flat-flat cavity was formed in the x–z plane.

Figure 8(a) shows the output power as a function of the pump power of the Nd:YVO_4 slab laser hybrid resonator. Because of the diffraction loss of fundamental mode and the machining error of resonator mirrors, a maximum output power of 117 W continuous-wave 1064 nm laser was obtained at a pump power of 328 W and showed no saturation. The corresponding O-O efficiency was 35% and the slope efficiency was 51%. The output beam has a size of about 1.1 mm ×4.0 mm. The beam quality at the full pump power of 328 W was measured by a beam quality analyzer (M2-200S, Spiricon Inc.), as shown in Fig. 8(b). The laser beam quality factors were measured to be 1.57 in the stable direction and 1.66 in the unstable direction. The upper inset in Fig. 8(b) shows the two-dimensional spatial intensity profile of the laser beam. The central wavelength and spectral width of output beam had almost no change after the ASE management.

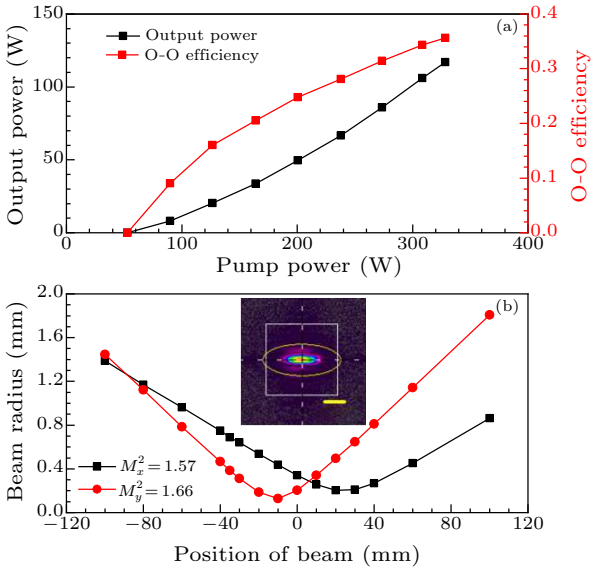

Fig. 8. (a) Output power versus the pump power. (b) The measured beam quality of the laser at the full pump. Upper inset: 2D spatial intensity profile of the laser beam.

Table 1. Typical Nd-doped homology crystal slab laser experiment results.

Crystal	Wavelength	Output power	M^2	Scheme	References
Nd:YVO_4	1064 nm	170 W	1.9 1.3	End-pumped	[18]
Nd:YVO_4	1064 nm	300 W	2.1 3.4	Innoslab	[3]
Nd:YVO_4	1342 nm	22 W	1.2 1.3	End-pumped	[19]
Nd:$GdVO_4$	1064 nm	120 W	2.3 2.3	Innoslab	[20]

In conclusion, to achieve the ASE management of the slab, we performed short-cavity experiments using different absorbing coatings. Three kinds of coatings completed 43, 65, and 153 W maximum output power, representing three management levels of ASE, respectively. Through changing the design of the coating structure, the thickness of the film, and the sequence of films, we can achieve the flexible change of coating absorptivity to manage the ASE in different situations. With a hybrid resonator and absorbing coatings, a 117 W continuous-wave 1064 nm laser was obtained with an absorbed pump power of 328 W at 888 nm and showed no saturation. The optical-to-optical efficiency and slope efficiency were 35% and 51%, respectively. The beam quality factors were measured to be 1.57 in the stable direction and 1.66 in the unstable direction.

References

[1] McDonagh L, Wallenstein R, Knappe R et al 2006 *Opt. Lett.* **31** 3297
[2] Zhu P, Li D J, Hu P X et al 2008 *Opt. Lett.* **33** 1930
[3] Xu L, Zhang H L, Mao Y F et al 2014 *Laser Phys. Lett.* **11** 115809
[4] Shen Y J, Gong M L, Ji E C et al 2017 *Opt. Commun.* **383** 430
[5] Waritanant T and Major A 2016 *Appl. Phys. B* **122** 135
[6] Sridharan A K, Saraf S, Sinha S et al 2006 *Appl. Opt.* **45** 3340
[7] Chen Z Z, Xu Y T, Guo Y D et al 2015 *Appl. Opt.* **54** 5011
[8] Goodno G D, Komine H et al 2006 *Opt. Lett.* **31** 1247
[9] Allen L and Peters G I 1973 *Phys. Rev. A* **8** 2031
[10] Jiao H F, He Y, Bao G H et al 2017 *Appl. Opt.* **56** C100
[11] Nguyen V B, Gubanova L A and Hoang T L 2018 *J. Opt. Technol.* **85** 53
[12] Lee T P, Burrus C A and Miller B I 1973 *IEEE J. Quantum Electron.* **9** 820
[13] Hall D C, Burns W K and Moeller R P 1995 *J. Lightwave Technol.* **13** 1452
[14] Dobrowolski J A, Li L and Kemp R A 1995 *Appl. Opt.* **34** 5673
[15] Sullivan B T and Byrt K L 1995 *Appl. Opt.* **34** 5684
[16] Xu L, Zhang H L, He J L et al 2012 *Appl. Opt.* **51** 2012
[17] Chen Y F, Lan Y P and Wang S C 2000 *Opt. Lett.* **25** 1016
[18] Mao Y F, Zhang H L, Xu L et al 2014 *Chin. Phys. Lett.* **31** 074206
[19] Zhang H L, Xu L, Cui L et al 2010 *Chin. Phys. Lett.* **27** 104212
[20] Deng B, Zhang H L, Xu L et al 2014 *Chin. Phys. Lett.* **31** 114201